

## Evolution of Coherent Vortex Structures in the two-dimensional Mixing Layer\*

*Li, W. C.<sup>1)</sup>, Fan, J. R.<sup>1)</sup>, Luo, K.<sup>1)</sup> and Cen, K. F.<sup>1)</sup>*

*1) Institute for Thermal Power Engineering and CE & EE, Zhejiang University, Hangzhou 310027, China.*

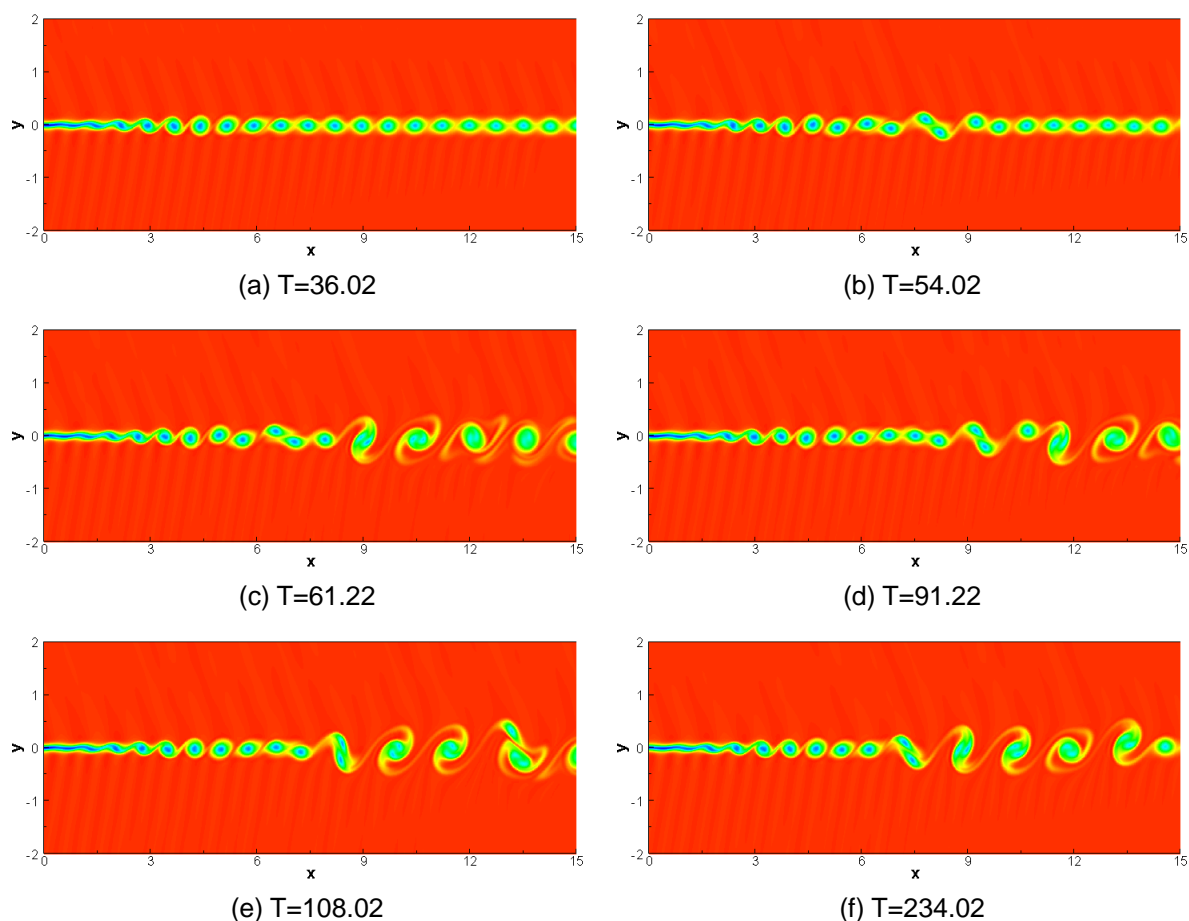


Fig. 1. The evolution of the vortex structures of mixing layer.

Using a DNS (direct numerical simulation) method, the vortex structures of a two-dimensional spatial developing mixing layer were simulated. And a two-dimensional perturbation to the mean, which was based on the unstable wavenumbers of the streamwise direction, was imposed initially. A non-uniform fourth-order compact finite difference scheme is utilized to evaluating the spatial derivatives. The Euler terms were marched in time using sufficient accuracy, low-storage, five-stage fourth-order Runge-Kutta integration scheme. But the viscous and conduction terms were marched in time using a first-order integration scheme reducing the computational time without loss of accuracy.

Fig.1 shows the evolution of the vortex structures in the flow-field. In (a), the ‘cat-eye’ vortex structures roll up, and from non-dimensional time  $T=54.02$ , as shown in (b), (c), (d), (e) and (f), the pairing process of vortexes begin, and captured precisely the pairing of two vortexes and the special mixing progress of three vortexes appearing in the free shear layer. Finally, the field develops in the direction of streamwise with topological sorting structure.

\* Supported by the National Natural Science Key Foundations of China (No. 50236030)

## Visualization of air flow and smoke spreading for realistic indoor-climate situations\*

*Kenjeres, S.<sup>1)</sup>, Gunarjo, S. B.<sup>1)</sup> and Hanjalic, K.<sup>1)</sup>*

*1) Department of Multi Scale Physics, Faculty of Applied Sciences, Delft University of Technology, Lorentzweg 1, 2628 CJ Delft, The Netherlands.*

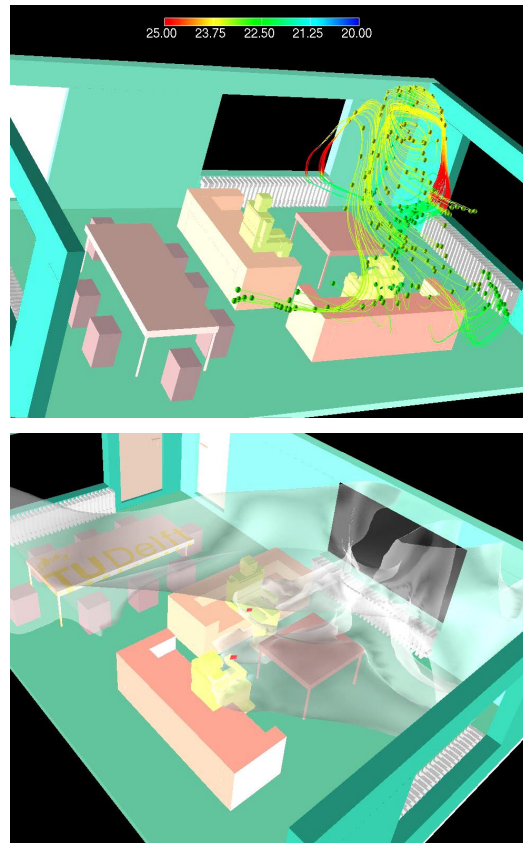


Fig. 1. Instantaneous trajectories of massless particles colored by local temperature revealing complex interactions between thermal jets (originating from the local thermally active sources - radiators) – above; passive scalar (smoke) distribution after 5 min – the smoke is released over two localized sources just above occupants hands-imitating two active smokers – below.

Numerical simulations of realistic indoor-climate situations (furnished and occupied office space with two active smokers) demonstrated that the time-dependent RANS (T-RANS) approach when combined with the passive-element treatment for representation of complex interior space can be used as a powerful tool for accurate predictions of air flow, scalar transport and wall-heat and mass transfer in complex buildings. The method can be regarded as Very Large Eddy Simulations (VLES) since the deterministic and modeled contributions to the turbulence moments are of the same order of magnitude. The simulated geometry is represented by  $122 \times 82 \times 82$  control volumes (clustered closely to the thermally active sources) and approximately 300 passive elements. The flow is buoyancy-driven with typical values of non-dimensional parameters:  $Ra=1.5 \times 10^{12}$ ,  $Pr=0.71$ .

\* Kenjeres, S., Hanjalic, K. and Gunarjo, S. B., "A T-RANS/VLES approach to indoor climate simulations", FEDSM2002-31400, Proc. ASME 2002 Fluids Engineering Division Summer Meeting, Montreal, Quebec, Canada, July 14-18, 2002.

## Visualization of High Speed Air Flow by the Spark Tracing Method with Radiant Trail

*Ninomiya, N.*<sup>1)</sup>, *Akiyama, M.*<sup>2)</sup>, *Sugiyama, H.*<sup>1)</sup> and *Katakami, A.*<sup>3)</sup>

1) Department of Energy and Environmental Science, Graduate School of Engineering, Utsunomiya University, 7-1-2 Yoto, Utsunomiya, Tochigi 321-8585, Japan.

2) Professor Emeritus, Utsunomiya University, 7-1-2 Yoto, Utsunomiya, Tochigi 321-8585, Japan.

3) Fuji Heavy Industries Ltd., 1-1, Subaru-cho, Ohta-shi, Gunma 373-8555, Japan.

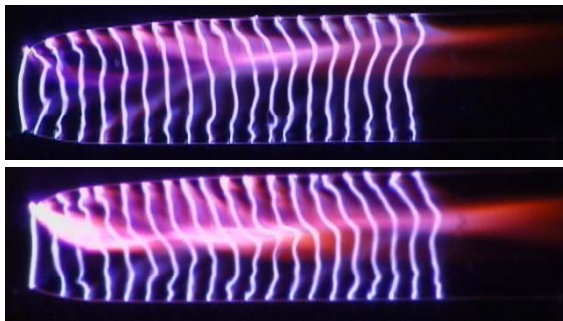


Fig. 1. Sparks with egg shell powder

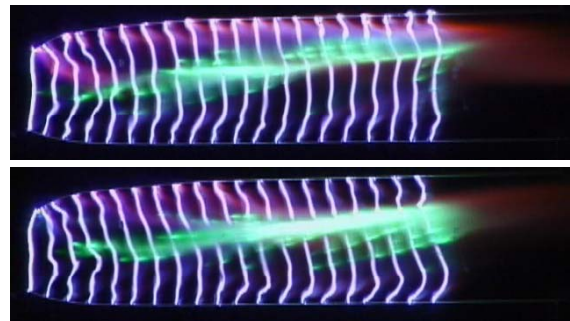


Fig. 2. Sparks with Copper powder.

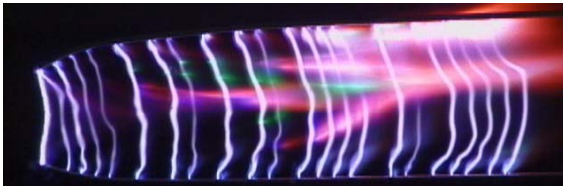


Fig. 3. Sparks with egg shell powder and Copper powder.

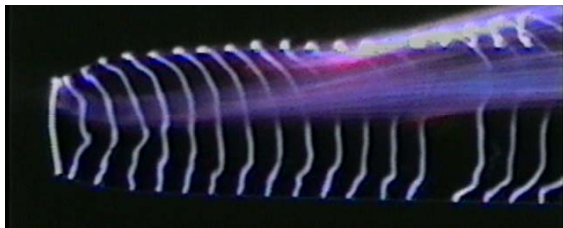
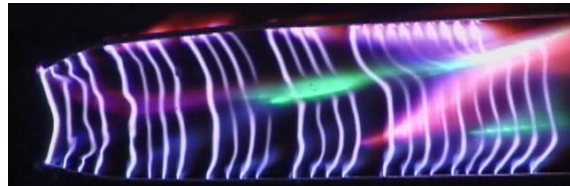


Fig. 4. Sparks with Aluminum oxide.

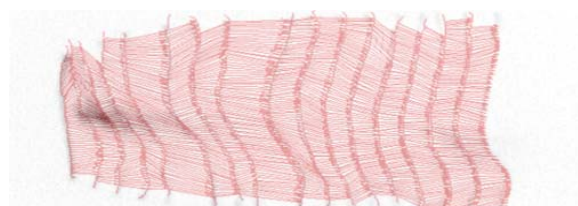
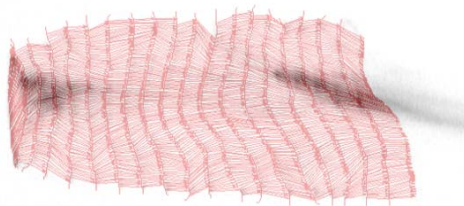
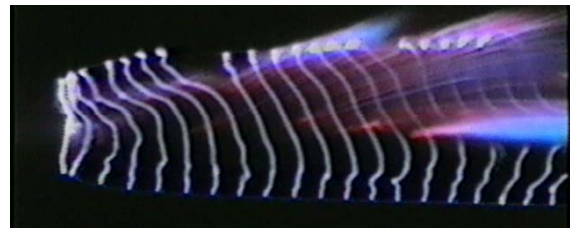


Fig. 5. DP matching results compared with radiant trail.

The spark tracing method is known as a convenient visualization technique for high speed air flow and the time lines can be obtained. Nevertheless, the transverse motion to the time lines is still under question. Presently, the metallic powder is introduced to the incoming air flow and thus the streak lines are also visualized as the radiant trail, which emerges when the powder is burned by the sparks. Calcium in the egg shell presents the red tail as in Fig. 1 and Copper looks green as in Fig. 2. The combination of these powders shows a colorful pattern (Fig. 3). The radiant trail by the fine powder of Aluminum oxide (Fig. 4) represents the detailed flow vectors, which compares very well with the Dynamic Programming matching results (Fig. 5).

## Visualization of Particle Dispersion by Vortex Structures with Direct Numerical Simulation\*

Zheng, Y. Q.<sup>1)</sup>, Fan, J. R.<sup>2)</sup> and Wu, P.<sup>1)</sup>

1) Associate Professor & Ph.D., Department of Mechanical Engineering, Zhejiang University of Science and Technology, Hangzhou, 310012, China.

2) Professor & Ph.D., Institute for Thermal Power Engineering, Zhejiang University, Hangzhou 310027, China.

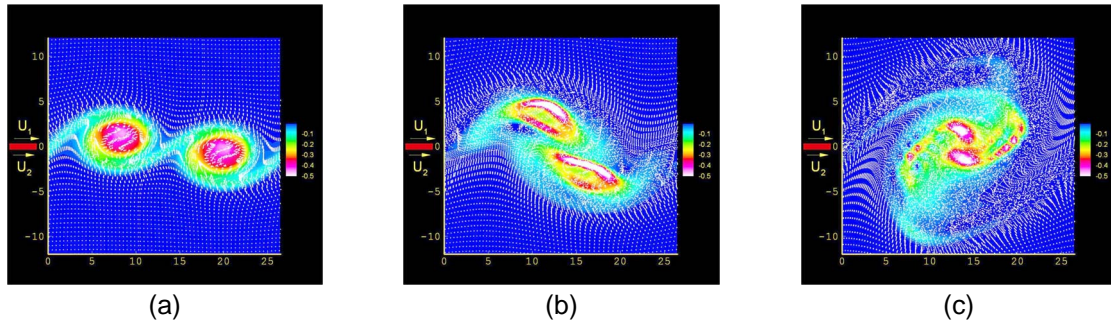


Fig. 1. The dispersion patterns with time for particles at  $St=0.01$ .

(a)  $T=35$ ; (b)  $T=60$ ; (c)  $T=85$

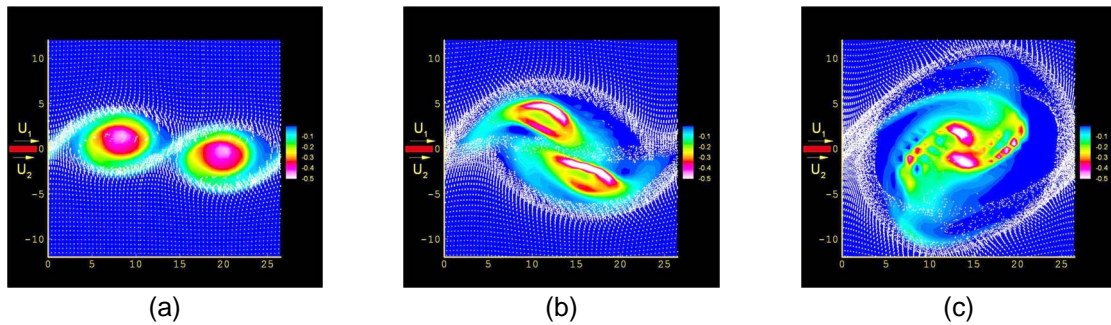


Fig. 2. The dispersion patterns with time for particles at  $St=5$ .

(a)  $T=35$ ; (b)  $T=60$ ; (c)  $T=85$

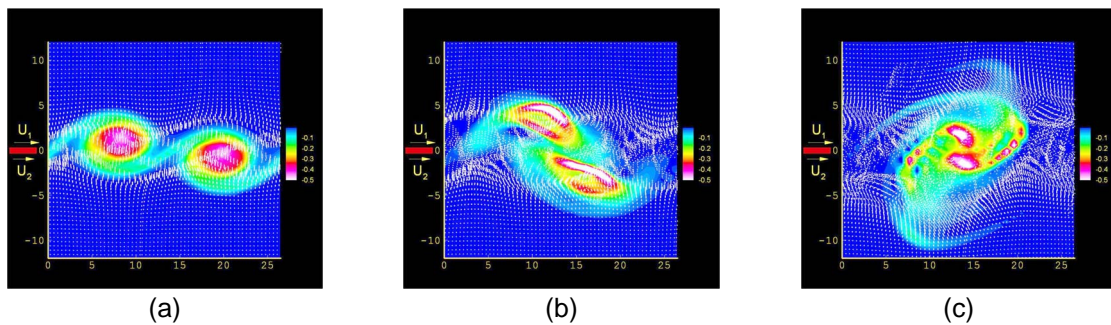


Fig. 3. The dispersion patterns with time for particles at  $St=100$ .

(a)  $T=35$ ; (b)  $T=60$ ; (c)  $T=85$

The particle dispersion with different Stokes numbers by the vortex structures in a turbulent mixing layer was directly simulated. The white dots in the figures represent the particles distribution, and the color contours represent the vortex structures. For small Stokes number (Fig. 1), the particles followed closely the turbulence of the fluid, however, for large Stokes number (Fig. 3), the fluid motion should have little effect on the particles. For particles with Stokes number of the order of unity (Fig. 2), the particles tendency to concentrate near the outer edges of the larger-scale structures was evident. The visualizations showed that the dispersion of particles was closely related to the large-scale organized structures.

\* Supported by Zhejiang Provincial Natural Science Foundation of China under Grant No. M503094, and Scientific Research Fund of Zhejiang Provincial Education Department under Grant No. 20030841.

## A Detailed 3D Model of the Human Hand

*Gehrmann, S. <sup>1)</sup>, Höhne, K. H. <sup>2)</sup>, Linhart, W. <sup>1)</sup>, Pommert, A. <sup>2)</sup>, Tiede, U. <sup>2)</sup> and Yarar, S. <sup>1)</sup>*

*1) Department of Traumatology, Hand and Reconstructive Surgery, University Hospital Hamburg-Eppendorf, Martinistr. 52, 20246 Hamburg, Germany.*

*2) Institute of Medical Informatics, University Hospital Hamburg-Eppendorf, Hamburg, Germany.*

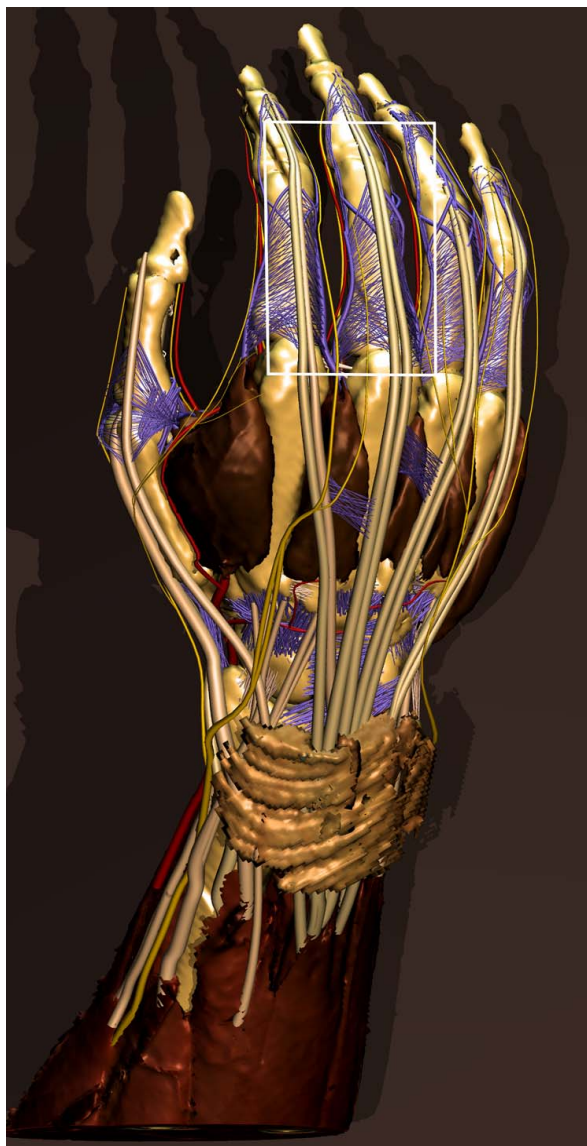


Fig. 1. Combined volume and surface model of the hand.

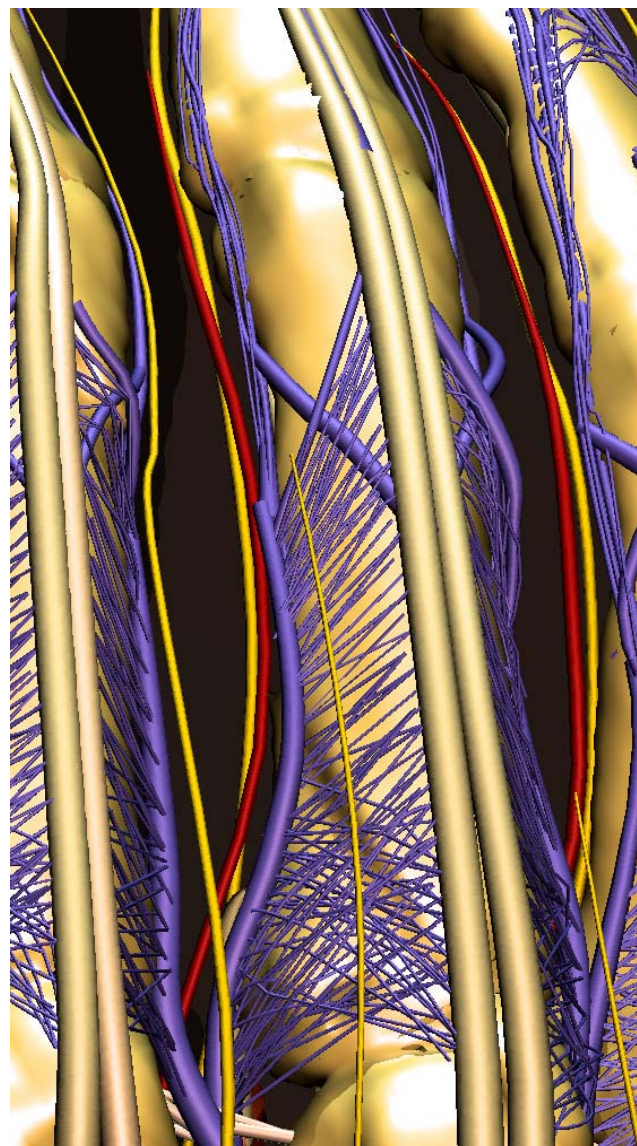


Fig. 2. Detail within the rectangle depicted in Fig. 1.

Because of its complicated anatomy and function, the human hand is a most delicate object for surgery. Therefore a tool for learning the detailed anatomy and the possibility of training surgical interventions without harm for a patient is highly desired. For this purpose the shown 3D model has been created from the Visible Human data set (Fig. 1). The large objects, like bone and muscles are volume objects, while the small objects such as blood vessels (red), nerves (yellow), tendons (gray) and ligaments (blue) are modelled as surface objects (Fig. 2). The model contains about 400 anatomical objects. Within the VOXEL-MAN framework it can be explored and interrogated by mouse click (e. g. “show me the branches of this nerve”). Tools for simulation of surgical interventions are under development.

## Camera visualization of cloud fields simulated by non-hydrostatic atmospheric models

Iwabuchi, H. <sup>1)</sup> and Tsuboki, K. <sup>1,2)</sup>

1) Frontier Research Center for Global Change, Japan Agency for Marine-Earth Science and Technology, 3173-25 Showa-machi, Kanazawa-ku, Yokohama, Kanagawa 236-0001, Japan.

2) Hydrospheric Atmospheric Research Center, Nagoya University, Furo-cho, Chikusa-ku, Nagoya, Nagoya 464-8601, Japan.

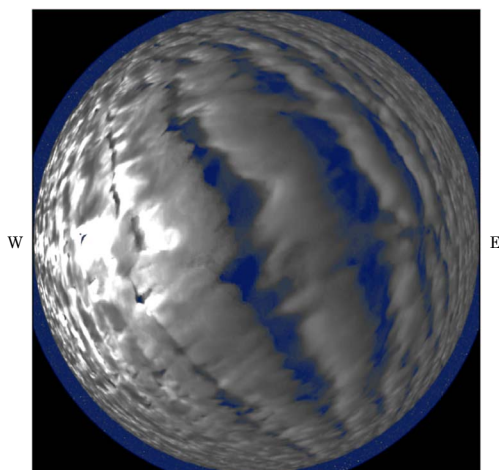


Fig. 1. A whole-sky camera image looking up from ground.

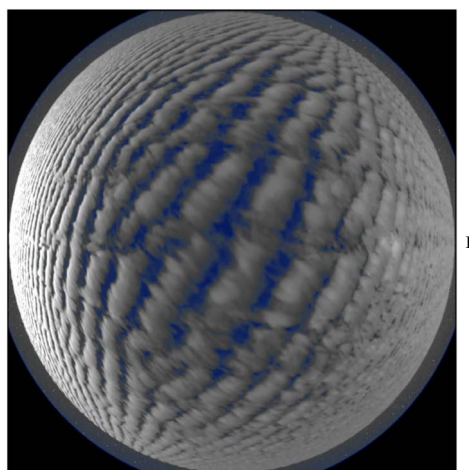


Fig. 2. As Fig.1, but looking down from 5 km above cloud top.

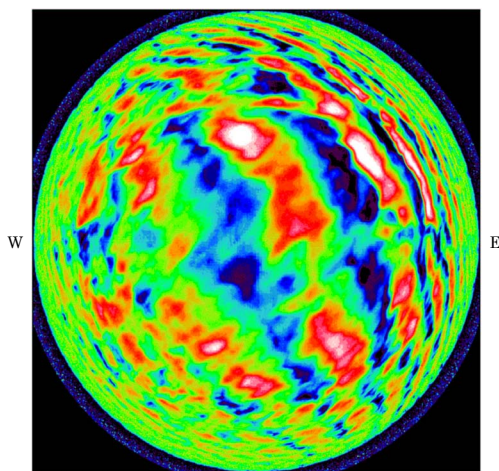


Fig. 3. As Fig.1, but for infrared camera.

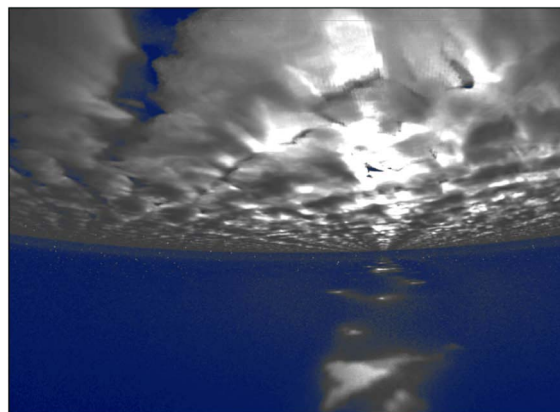


Fig. 4. Wide-angle camera image pointed at 10 degrees elevation angle and 20 degrees south of west, from 400 m above the ocean surface.

These figures show simulated camera images of marine stratocumulus clouds, which were realized by a non-hydrostatic atmospheric model, CReSS (Cloud Resolving Storm Simulator). The solar elevation is 30 degrees, and the sun is in the west. Monochromatic radiances at visible and infrared wavelengths were simulated by a three-dimensional radiative transfer model, which was based on the Monte Carlo photon-transport algorithm. Characteristics such as bright cloud edges near the sun and dark shadowed sides are consistent with human experiences. Reality of the visualized clouds depends solely on how well the cloud-resolving model represents physical processes, because the visualization using the radiation model is highly accurate.